Topology characteristics of liquid ammonia swirl spray flame

Ruixiang Wang [a], Meng Zhang [a],*, Zhenhua An [b], Xiao Cai [a], Jiawen Liu [a], Jinhua Wang [a], Zuohua Huang [a]

[a] State Key Laboratory of Multiphase Flow in Power Engineering, Xi'an Jiaotong University, Xi'an 710049, China
[b] Department of Mechanical Engineering and Science, Kyoto University, Kyoto daigaku-Katsura, Nishikyo-ku, Kyoto 615-8540, Japan

ARTICLE INFO

ABSTRACT

The utilization of liquid ammonia in gas turbines can reduce energy loss and start-up time. However, the flash boiling phenomenon and the high latent heat of liquid ammonia make the spray flame difficult to stabilize. Increasing the preheated air temperature or adding a small amount of hydrogen as a piloted fuel are considered as effective methods to enhance the stability. To understand the flame topological structure, simultaneous Mie scattering and planar laser-induced fluorescence of OH (OH-PLIF) techniques were used to visualize the liquid ammonia spray structure and flame region information. Results show that the liquid ammonia swirl spray flame exhibits the flame topological structure of distinct zoning characteristics, including the droplet zone, the mixing zone, and the flame zone. Increasing the preheated air temperature accelerates the evaporation of liquid ammonia, leading to an increase in the local equivalence ratio and radial flame splitting. At lower air temperature conditions, increasing the hydrogen blending ratio has minimal impact on the flame topological structure. However, at higher temperature conditions, hydrogen blending significantly promotes reaction intensity upstream and reduces the flame lift-off height, which makes the mixing zone smaller. In general, to achieve a better flame stability effect, the two factors need to be reasonably matched, which has important reference value for the development of liquid ammonia fueled gas turbine combustors.

1. Introduction

Ammonia (NH$_3$) is increasingly being considered as a potential alternative to traditional hydrocarbon fuels in zero carbon fuel systems [1], and it has received significant attention due to its well-established infrastructure, low cost, and potential as a hydrogen carrier [2]. Therefore, the large-scale application of NH$_3$ in power equipments such as gas turbines (GTs) can not only reduce the greenhouse effect but also alleviate the energy crisis from the combustion side.

In recent years, extensive researches have been conducted on the gas-phase ammonia combustion GT's combustors. The stability of ammonia combustion flames has been a key focus of study due to its lower flame speed and heat release rate. Hayakawa et al. [3], Wei et al. [4,5], Kurata et al. [6] successfully achieved stable combustion of pure ammonia flames in swirl combustors. Zhang et al. [7], Khateeb et al. [8], Franco et al. [9] Elbaz et al. [10] studied the enhancement of ammonia flame stability through the use of small molecule reactive fuels such as H$_2$ and CH$_4$ blending.

However, ammonia is typically stored in liquid form which has much higher volume energy density compared to gaseous ammonia. Particularly in GT's applications, using gaseous ammonia for combustion requires the installation of evaporators, accumulators, and heating lines in the supply pipeline to prevent ammonia condensation, resulting in 7%–9% energy loss and prolonged start-up time. Direct injection of liquid ammonia in gas turbines can save the energy required for pre-evaporation, simplify the equipment in the system, and reduce start-up time, making it a new research focus due to these advantages.

Currently, many scholars have conducted research on liquid ammonia spray and combustion, particularly in internal combustion engines (ICEs) [11–14]. However, the research on direct liquid ammonia combustion in gas turbines is still limited. Regarding the continuous spray characteristics of liquid ammonia, Colson et al. [15] characterized the effect of injection temperature and nozzle geometry on the spray characteristics and the transition from normal evaporation to flashing. They found that the flash boiling phenomenon and the nozzle structure have significant effects on the spraying characteristics of liquid ammonia, such as spray angle and penetration distance. Okafor et al. [16] used a hollow cone nozzle to generate a continuous spray of liquid ammonia and measured temperature variations along the direction of the spray. Their study showed that due to flash boiling and high latent heat of vaporization of liquid ammonia, the surrounding air temperature decreased rapidly to about 223 K after injecting liquid ammonia into the combustion chamber under non-reactive condition. Regarding the

---

* Corresponding author.
  E-mail address: mengz8851@xjtu.edu.cn (M. Zhang).

combustion of liquid ammonia in swirl spray applications, Okafor et al. [16,17] employed a novel single-stage model gas turbine swirl combustor and a two-stage combustor to stabilize liquid ammonia and methane co-firing flame successfully and studied the flame stability and emission characteristics. Their study showed that co-firing the liquid ammonia spray with methane or increasing preheated air temperature can improve the stability of the spray flame and extend the blow-off limits. Somarathne et al. [18] simulated 100% liquid ammonia swirl spray flame. They found that accounting for flash boiling to equilibrium evaporation at moderately high pressures is essential, and liquid ammonia spray flames can be stabilized using preheated swirling airflow. Masahiro et al. [19] conducted a demonstration test using a liquid ammonia fueled 2 MW-class gas turbine using methane blending, and evaluated the performance of the combustor. They found that liquid ammonia achieved stable combustion and co-firing with methane could suppress unburned ammonia emissions. Yamashita et al. [20] studied the injection and combustion characteristics of liquid ammonia under non-reactive and reactive conditions and found that increasing the preheated air temperature can widen the combustion limits of the liquid ammonia swirl spray flame. These researchers have all pointed out the feasibility of using liquid ammonia in gas turbine applications.

Nonetheless, the stability issue faced by gaseous ammonia is still a concern for liquid ammonia swirl spray flames. In particular, the flash boiling of liquid ammonia exacerbates local heat loss, making the flame more difficult to stabilize. Increasing preheated air temperature and blending small molecule reactive fuels are considered as important means to stabilize liquid ammonia swirl spray flames and they also have an impact on the flame topological structure. Understanding the flame topological structure is crucial in studying the stability of spray flames [21,22]. However, the research on liquid ammonia swirl spray flame is very limited and the flame topological structure is unclear since the flame contains a strong flash boiling process.

To this end, this study investigates the topological structure of liquid ammonia spray swirl flames and discusses the influence of preheated air temperature and hydrogen blending ratio on the flame topological structure. The remainder of the present work is organized as follows. The topology of the liquid ammonia swirl spray flame is presented in Section 3.1. The impact of preheated air temperature and hydrogen addition is presented and discussed in Section 3.2. The last Section 3.3 analyzes the statistical results.

2. Experimental methods

Fig. 1 shows the schematic diagram of the liquid ammonia supply system and the liquid ammonia swirl spray burner. Liquid ammonia (LNH_3) with purity larger than 99.9% was pumped from a 100 kg LNH_3 tank to the supply system and went through a water bath at the temperature of 268 K (−5 ℃) to keep its liquid phase. Then LNH_3 was pressurized to above 4.0 MPa through a constant flow pump to the high-pressure tube section, as indicated by the red pipeline in the diagram. A back pressure valve was installed to connect the high and low-pressure sections and to release the pressure once it goes above the set value. In the experiments, the LNH_3 mass flow rate was steadily controlled at 0.4 g/s. The temperature and pressure just ahead of the burner were stabilized at 274 K and 4.30 MPa which was verified to keep the ammonia in liquid phase.

In the liquid ammonia swirl spray burner, a 60°pressure-atomizing hollow cone nozzle (Lechler 220.014) was installed on the center spray rod of the burner to generate stable liquid ammonia spray. Hydrogen was supplied through an annular gap with a width of 1 mm around the nozzle. Preheated air was injected tangentially through 8 rectangular (4.39×10 mm^2) shaped slits of a radial swirler and exited the swirler axially through the 30 mm diameter swirler exit. The swirl number calculated with $S = \pi R^2 / A_s$ is equal to 2.01 [16]. Here, R is the swirler exit radius (15 mm) while A_s is the total area of the swirler inlet slits. At six different positions in the combustion chamber, an OMEGA

Table 1
Preheated air temperature (T_{air}) and the heat fraction of ammonia for the 9 operating conditions. T378E96 indicates that T_{air} = 378 K and E_{NH_3} = 0.96.

T_{air} E_{NH_3}	378 K	428 K	478 K
1.00	T378E100	T428E100	T478E100
0.96	T378E96	T428E96	T478E96
0.92	T378E92	T428E92	T478E92

type K unsheathed thermocouple (CHAL-032) was used to obtain high-frequency measurements, with a probe diameter of 0.81 mm, and a standard error of ±1.5 ℃ at −40–375 ℃ and 0.4% at 375–1000 ℃.

The fraction of ammonia in the fuel in this study is expressed in terms of the heat fraction of ammonia, E_{NH_3}.

$$E_{NH_3} = \frac{x_{NH_3} LHV_{NH_3}}{x_{NH_3} LHV_{NH_3} + x_{H_2} LHV_{H_2}} \tag{1}$$

Here, x_{NH_3} and x_{H_2} are mole fractions of NH_3 and H_2 in a binary fuel and LHV stands for the lower heating value (LHV_{H_2} = 242 kJ/mol, LHV_{NH_3} = 317 kJ/mol).

In this study, the heat fraction of ammonia was set to 0.92, 0.96, and 1.00. The air was preheated by a 40 kW heater, and the air temperature was measured upstream of the swirler to confirm that the thermal radiation from the flame does not affect the measurement. The air temperatures were designed to be 378 K, 428 K, and 478 K. Actual temperature fluctuation was maintained within ±2 K. All possible combinations of preheated air temperature and the heat fraction of ammonia lead to nine operating conditions which are listed in Table 1. The global equivalence ratio ϕ is calculated using both ammonia and hydrogen and is set at ϕ = 0.9 for all operating conditions. Air and fuel flow rates were controlled using mass flow controllers, with an uncertainty of ±1% of the set point. Therefore, uncertainties of the bulk velocity and ϕ are about ±0.023 m/s and ±1.0%, respectively.

Direct flame photographs were taken with a Canon EOS Kiss X5 camera with a shutter gate of 1/1600 s. NH* chemiluminescence images were recorded at 10 Hz with an ICCD camera (LaVision ProX + IRO) equipped with a UV lens (f.l. = 105 mm, f/5.6) and a bandpass filter of 340 ± 11 nm. NH* chemiluminescence images were averaged over 10 s and are presented after an inverse Abel transform.

The simultaneous Mie scattering and OH-PLIF measurements were performed to detect the liquid spray and combustion. A YAG laser was used to produce a 532 nm beam (160 mJ/pulse) for the Mie scattering signal. A Quantel Qsmart 1500 YAG laser (10 Hz) and a Quantel Qscan dye laser were used to generate 283 nm laser (16 mJ/pulse) for OH Planar Laser-Induced Fluorescence (OH-PLIF) signal. The 532 nm laser and 283 nm laser were combined and formed laser sheets with a height of approximately 90 mm, and thickness of 1.5 mm and 0.5 mm, respectively. The Mie scattering signal was captured by a CCD camera (LaVision SX 6M) equipped with an optical lens (f.l. = 100 mm, f/2.8) and a bandpass filter of 532 ± 10 nm. The OH-PLIF signal was captured by an ICCD camera (LaVision ProX + IRO) equipped with a UV lens (f.l. = 105 mm, f/5.6) and a bandpass filter of 310 ± 10 nm. The window size of Mie scattering and OH-PLIF is 2752 × 2200 and 1600 × 1200, with resolutions of approximately 0.035 mm/pixel and 0.080 mm/pixel respectively. The actual window size on the combustion chamber is 70 mm in width and 80 mm in height.

Both Mie scattering and OH-PLIF images were transformed to be spatially aligned with each other on a pixel-by-pixel basis. The images were further processed via Matlab with background subtraction, 3 × 3 median filtering, and a threshold below which the signal was put to zero. The Mie scattering × OH was then plotted as an indicator of the droplet zone and flame zone. 500 images were recorded for each operating condition.
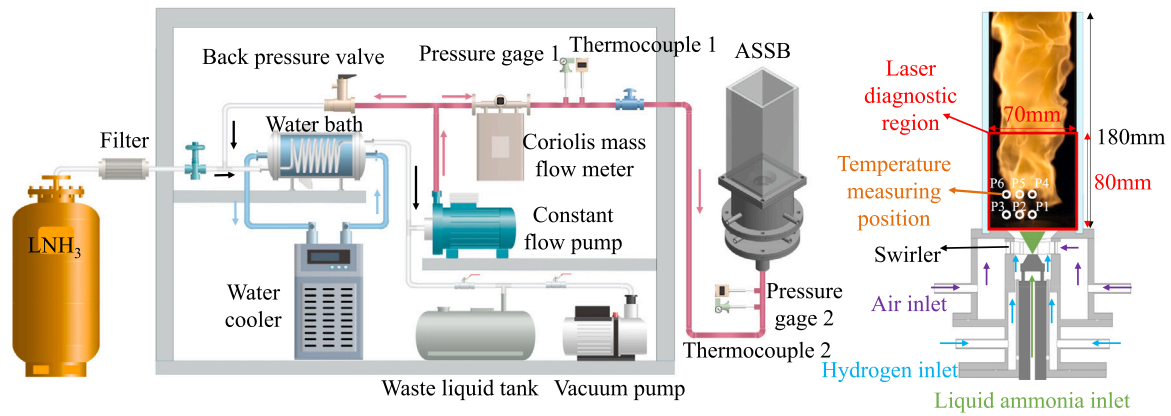
Fig. 1. Schematic diagram of the liquid ammonia supply system and the liquid ammonia swirl spray burner (ASSB).
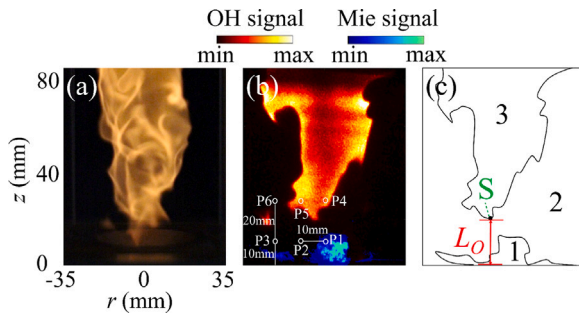

Fig. 2. (a) Flame photo, (b) simultaneous Mie scattering and OH-PLIF images and (c) boundaries for different zones. The operating condition is T378E100. The distance between the lowest point of the OH signal boundary (S) and the burner exit plane is defined as the flame lift-off height (L_o) [22]. The positions of the temperature measurement points P1–P6 are shown in (b).

Fig. 3. The temperature fluctuation with time at six measurement locations under the condition of T378E100. The measurement positions are indicated in Fig. 2. The measurement was performed at 1 kHz beyond 100 s.

3. Results and discussion

3.1. Typical topological structure

The typical feature of instantaneous liquid ammonia spray flame is illustrated by the flame photos, as shown in Fig. 2(a), and the simultaneous Mie and OH-PLIF signals as shown in Fig. 2(b). After the image binarization of Fig. 2(b) and extracting the boundaries to obtain Fig. 2(c), we can see that the overall flame topology exhibits clear zoning characteristics, with the Mie signal area considered as the liquid droplet zone 1 and the OH-PLIF signal area as the flame zone 3. The area off zones 1 and 3 with no signals is considered as zone 2.

The topological structure of the liquid ammonia swirl spray flame is considered to include the initial stage of liquid ammonia spray, the evaporation process (liquid droplet zone), followed by the mixing process of gaseous ammonia and air (mixing zone), and finally the stable combustion process (flame zone). Fig. 3 shows the temperature fluctuation over 100 s at six different positions (indicated in Fig. 2(b)) under the condition of T378E100. It can be observed that the averaged temperature at the height of $z = 10$ mm is relatively low with smaller fluctuations, indicating the liquid droplet zone. The lower temperature at this height is mainly attributed to the less amount of recirculated hot gas and the flash boiling phenomenon of the liquid ammonia droplets. At $z = 30$ mm, the averaged temperatures at $r = 0$ and $−10$ mm are higher with larger fluctuations, representing the mixing zone, where the evaporation and combustion of the spray alternately occur, visually manifesting as flame flickering or pulsating. Since this area is closer to combustion downstream, the averaged temperature is relatively high, i.e. about 700 °C. However, due to the random occurrence of droplets and flame in this region, the temperature fluctuation is larger. The
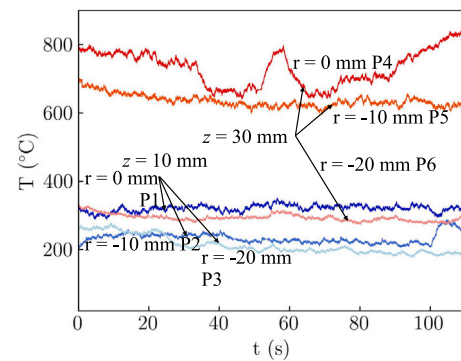
position of $z = 30$ mm and $r = -20$ mm is considered in the outer recirculation zone, showing the same level of temperature as $z = 10$ mm.

3.2. Effects of preheated air temperature and hydrogen addition

Fig. 4 shows the impact of preheated air temperature and hydrogen addition on the flame topological structure. It is found that adjusting the preheated air temperature and the heat fraction of ammonia will lead to significant and distinct changes in the topological structure in different ways. However, it can be seen that all operating conditions in Fig. 4 exhibit a similar flame topological structure as described in Fig. 2(b), with clear division of the different zones. Generally, there is no overlap region between the liquid droplet zone and flame zone. This is also a distinct characteristic that distinguishes the topological structure of the liquid ammonia spray flame from other liquid fuels without the flash boiling phenomenon [21].

Next, from the perspective of flame topological, the effects of temperature and hydrogen addition are discussed. When $E_{NH_3} = 1$, as T_{air} gradually increases from 378 K to 478 K, the droplet zone (Mie scattering signal) continually shrinks to a smaller area. This can be explained that hotter air causes more rapid ammonia droplets evaporation, which will lead to a more stable flame and an extension of the blow-off limits, as demonstrated in [16,17]. Due to the large latent heat of liquid ammonia, stable evaporation can be an important factor in stabilizing the spray flame since the local temperature exhibits large fluctuation resulting in local extinction. In addition, the OH signal near the central axis of the combustion chamber gradually weakens and the flame exhibits a split character as indicated in Fig. 4(g). This can be understood that a richer mixture is formed in the center of the flame
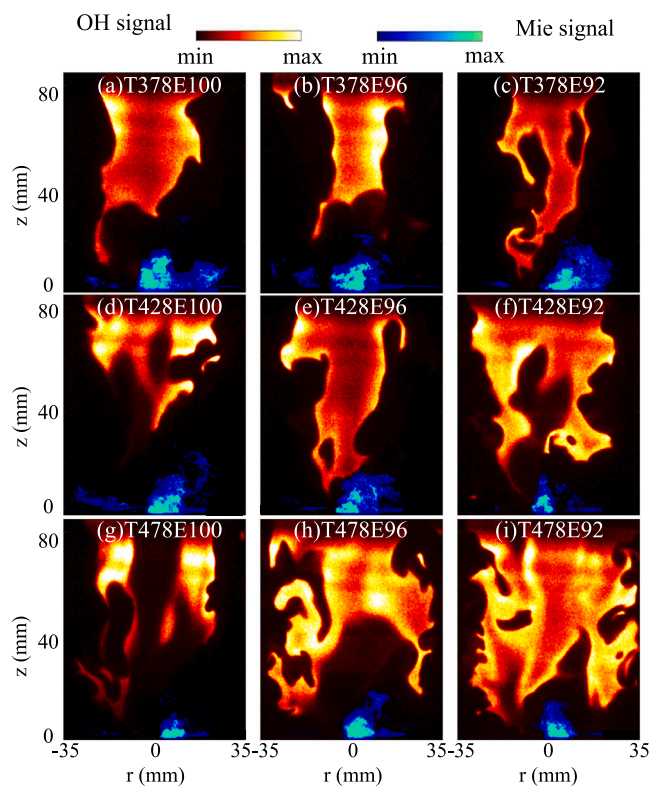
Fig. 4. Simultaneous Mie scattering and OH-PLIF signals for five typical operating conditions. Different rows exhibit the T_{air} effect and different columns exhibit the hydrogen addition effect.

Fig. 5. Flame photos (a–c) and the normalized time-averaged NH* images (d–f).

as T_{air} increases and the combustion occurs at the edge of the mixing zone. By further surveying the images, there is no visible difference in the distance between the OH signal and the Mie scattering signal.

When increasing T_{air} at E_{NH_3} = 0.96, besides the droplet zone shrinking as in the case of E_{NH_3} = 1, it can be seen that the OH distribution is extended in a transverse direction indicating larger flame area. The OH distribution is even extended at E_{NH_3} = 0.92, observing that the OH signal is full of the combustion chamber for the case of T478E92.

On the effect of hydrogen addition on ammonia flames, Awad et al. [23] indicated that the laminar flame velocity of hydrogen is much higher than that of ammonia (5–13 cm/s), so hydrogen addition can significantly increase the reactivity of ammonia flames, and the preferential diffusion effect of hydrogen leads to a much higher combustion intensity. Wei et al. [5] added 10% hydrogen to an ammonia/air swirl flame and found that the flame showed greater resistance to stretching and had fewer large-scale wrinkles and more small-scale wrinkles at the flame front, and an increase in the H, NH, and NH$_2$ fractions at the root of the flame, suggesting an increase in combustion intensity, which contributed to flame stabilization. Referring to the existing literature, the addition of hydrogen to a liquid ammonia swirl spray flame is supposed to have an enhancing effect on the flame.

However, in Fig. 4, it can be observed that the effect of hydrogen addition is largely dependent on the preheated air temperature when comparing the images in different columns. When T_{air} = 378 K, the topological structure of the swirl spray flame barely changes when increasing the hydrogen ratio, as illustrated from Fig. 4(a) to (c). The areas of the droplet zone are similar for three hydrogen ratios, indicating that the evaporation processes for the three cases are equivalent at this preheated air temperature. This can be understood that liquid ammonia evaporation is limited at T_{air} = 373 K and there are not enough unburned mixtures of gaseous ammonia and air for combustion.
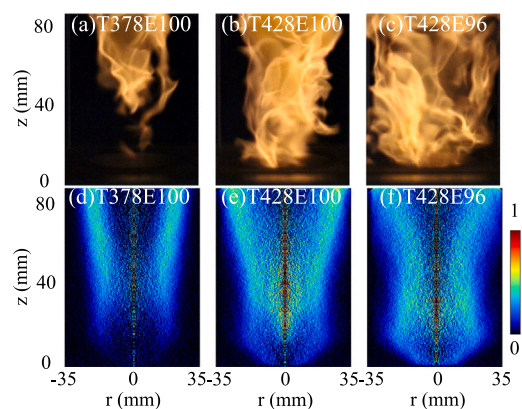
Nevertheless, it can be observed that the flame lift-off height seems to be shortened which is attributed to the addition of highly combustible hydrogen, igniting the ammonia near the flame base.

When T_{air} = 428 K, the evaporation process is enhanced and there is more gaseous ammonia. In this case, 4% hydrogen addition largely enhances the flame, by strengthening the flame base and shortening the flame lift-off height. The enhancement of the flame area from Fig. 4(b) and (e) is attributed to the addition of highly combustible hydrogen, igniting the originally ammonia-rich zone. Overall, to better stabilize the liquid ammonia swirl spray flame, the preheated air temperature and the addition of hydrogen need to be coordinated and regulated in conjunction with each other. As shown in the figure, the enhancement on combustion is even significant when T_{air} = 478 K, as shown from Fig. 4(g) and (i).

In summary, increasing T_{air} largely speeds up the evaporation process which has a direct influence on liquid ammonia swirl spray flame. The impact of preheated air temperature on the flame topological structure is not a linear change, as at higher preheated air temperature, the flash boiling of liquid ammonia becomes more severe, leading to excessively rich local equivalence ratios. In comparison, hydrogen addition provides more key radicals near the flame base while its effects on flame are largely dependent to T_{air}. As demonstrated by the above analysis, the preheated air temperature and the addition of hydrogen need to be coordinated and regulated in conjunction with each other to obtain a better liquid ammonia swirl spray flame.

To further clarify the two effects described above, NH* was also examined. Fig. 5 depicts the photos and the normalized time-averaged NH* images for different operating conditions. NH* can be regarded as an indicator of the reaction zone of the ammonia combustion [24]. It can be observed that by increasing T_{air} from 378 K to 428 K, the chemical reaction at the flame base is enhanced as indicated by the digital photographs, and the NH* signals. When considering hydrogen addition, the digital photograph in Fig. 5(b) and (c) shows a significant increase in the width of the flame base, with the flame approaching closer to the combustion chamber wall, corresponding to the outward expansion trend of the NH* base signal, as presented in Fig. 5(e) and (f). This can be understood as the further enhancement of the reaction at the flame base. These phenomena indicate that increasing the preheated air temperature and adding hydrogen both can enhance the reaction at the base of the flame.

The sum of the NH* intensity along the z direction was calculated for conditions in Fig. 6 to quantitatively reflect the positional information of the reaction zone. We note that increasing the preheated air temperature enhances the intensity of the reaction zone across the flame, with an average increase in NH* intensity of 89.51% in the z = 0–80 mm height range, comparing the T378E100 and T428E100 cases. The addition of hydrogen particularly enhances the chemical
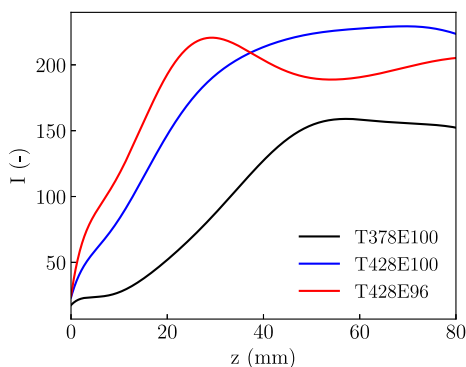
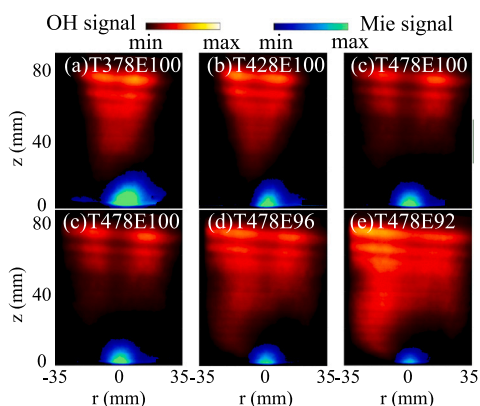**Fig. 6.** NH* intensity at different heights in the Z-direction.

Fig. 7. Mean images of the simultaneous Mie scattering signal and OH-PLIF signal. The first row examines T_{air} effects at $E_{NH_3} = 1$ and the second row examines hydrogen addition effects at T_{air} = 478 K.

Fig. 8. OH signal's lowest points (S) distribution. Five hundred data points are analyzed for S in each operating condition. The data is colored with the probability of the occurrence of point S. The first row examines T_{air} effects at $E_{NH_3} = 1$ and the second row examines hydrogen addition effects at T_{air} = 478 K.

reaction near the bottom of the flame, increasing the NH* intensity by an average of 34.03% in the $z = 0$–30 mm height range comparing the T428E100 and T428E96 cases.

Fig. 7 shows the mean Mie and OH signal images. In Fig. 7, as the preheated air temperature increases, there is no significant change in the flame zone structure from (a) to (b). However, from (b) to (c), a clear flame-splitting phenomenon occurs, and the droplet zone is reduced. Additionally, from (c) to (e), the addition of hydrogen blending markedly enlarges the flame zone and enhances the base of the flame, leading to a reduction in flame lift-off height, while the droplet zone is reduced and more concentrated at the burner exit. This suggests that to achieve a better liquid ammonia spray flame, these two factors need to be reasonably combined. This is consistent with the analysis in Fig. 4.

3.3. Statistical analysis

Based on the definition of point S in Fig. 2(c), Fig. 8 illustrates the distribution of point S for five operating conditions to further examine the effects of T_{air} and hydrogen addition. The flame lift-off height (L_o) can be defined as the distance of point S from the burner exit plane [22]. Because the liquid ammonia swirl spray flame exhibits distinct zoning characteristics, L_o can be used as the parameter of the topological features of the liquid ammonia swirl spray flame, allowing for the quantification of the flame zone position.

From Fig. 8(a) to (c), as T_{air} increases, the probability of the S point near the central axis of the combustion chamber gradually decreases. The position with the most probability of the S points appears near the chamber wall. From Fig. 8(c) to (e), with increasing hydrogen addition,
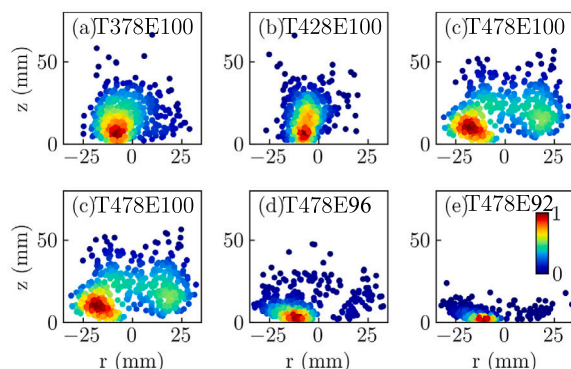
the S point is still near the wall but is generally closer to the outlet plane of the combustion chamber. The variation in the position of point S indicates that an increase in preheated air temperature causes the flame base, originally near the central axis of the burner, to split and move closer to the wall, while hydrogen blending stabilizes the base and reduces its lift-off height. This also confirms the inference made in the analysis in Fig. 4. When inspecting L_o, it is found that increasing T_{air} does not change the value of L_o, which means T_{air} does not alter the spatial distribution of the flame zone along the axial direction of the burner. On the other hand, increasing the hydrogen addition significantly reduces L_o, indicating that the flame area will be closer to the burner exit plane.

For the topological structure of liquid ammonia swirl spray flame, not only the location information is important, but also the area information. The previous analysis indicates that the region between the liquid droplet zone and the flame zone is primarily where ammonia and air are mixing. Fig. 9 shows the probability density distribution of the proportion of no-signal area to total image area, for the five operating conditions in Fig. 4. It can be observed that as T_{air} is increased from 378 K to 428 K, the Probability Density Function (PDF) profiles of the no-signal area are almost the same, meaning that the statistics of the mixing zone for these two cases are similar. However, when the air temperature is from 428 K to 478 K, the peak value remained the same, but the distribution became wider. From T478E100 to T478E92, the peak of the no-signal area shifts to the left, while the peak of the OH area shifts to the right, with the uniformity of the distribution curves remaining largely unchanged.

In terms of topological structure, increasing the preheated air temperature does not significantly change the size of the most frequently occurring flame area, rather, the probability of this area occurring decreases slightly. However, after adding hydrogen, the most frequently occurring flame area noticeably increases, and the probability of this area occurring remains largely unchanged.

This means that increasing the preheated air temperature does not effectively reduce the area of the mixing zone while adding a small amount of hydrogen can significantly reduce the area of the mixing zone. This further emphasizes the need for a coordinated approach between these two factors to better stabilize the liquid ammonia spray flame.

From the perspective of area information, in addition to the area of the mixing zone, the PDF of the overlapped area of the Mie and OH signals is calculated in Fig. 10. Firstly, it is noted that there is little probability of overlap between the two signals. It is observed that in the T478E100 condition, there is a very high probability that the droplet area and the flame area will not overlap, while increasing the preheated air temperature and hydrogen blending both increase the probability of
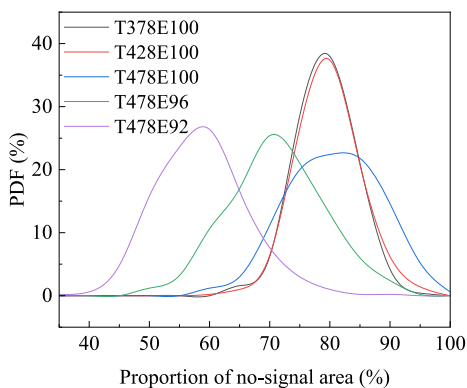
Fig. 9. The probability density function (PDF) of the proportion of the no-signal area, obtained from the 500 merged binary images for each condition.
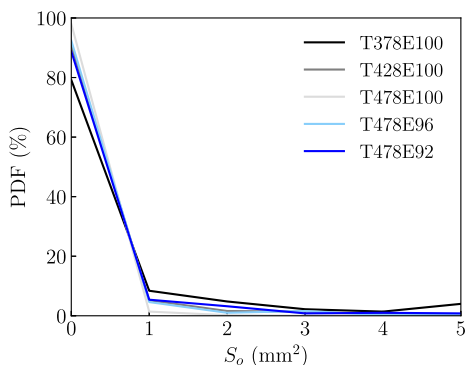

Fig. 10. The probability distribution function (PDF) of the overlap area (S_o) between the droplet zone and the flame zone.

overlap. Secondly, it is found that the area of overlap is the smallest for the T478E100 condition, and the largest for T378E100.

This phenomenon is primarily determined by the topological structure of the liquid ammonia swirl spray flame, as its structure zoning is very distinct, resulting in a rare overlap between the flame zone and the droplet zone. Furthermore, the increase in preheated air temperature causes the flame zone to split, thereby reducing the overlap area.

4. Conclusions

In this study, stable combustion of pure liquid ammonia swirl spray was achieved at 378 K, and the flame topological characteristics were observed. The influence of preheated air temperature and hydrogen blending on the flame topological structure was investigated. The research results lead to the following summaries and conclusions.

1. The flame topological structure of the liquid ammonia swirl spray exhibits distinct zoning characteristics, namely the liquid droplet zone, mixing zone, and flame zone.

2. The effects of preheated air temperature and hydrogen blending on the flame topological structure are different. Increasing the preheated air temperature causes the radial splitting of the flame zone, but does not change the axial height or the area of the flame zone. On the other hand, increasing hydrogen blending significantly increases the area of the flame zone and brings the flame zone closer to the burner exit plane, stabilizing the base of the flame near the burner exit.

3. The impact of preheated air temperature on the flame topological structure is not a linear change. At higher preheated air temperature, the flash boiling of liquid ammonia becomes more severe, leading to

excessively rich local equivalence ratios. Therefore, for better stabilization of the liquid ammonia swirl spray flame, a rational adjustment of the preheated air temperature and hydrogen addition is necessary.

4. The general characteristics of topological structure of the liquid ammonia swirl spray flame does not change with variations in the preheated air temperature or hydrogen addition. Overlapping between the droplet area and the flame area is very rare, distinguishing it from the spray combustion structure of traditional liquid fuels.

Novelty and significance statement

The novelty of this research lies in comprehensively investigating the topological structure characteristics of liquid ammonia swirl spray flames and employing laser diagnostic methods to analyze the characteristics of the droplet zone and the flame zone. This research is significant because it discovered the zoning structure of the flame, which distinguishes liquid ammonia from traditional liquid fuels, and revealed the influence patterns of preheated air temperature and hydrogen blending on the flame topological structure. These two factors not only affect the position of the flame base but also the area of various zones within the flame. The importance of this work lies in providing valuable insights into the stability of liquid ammonia swirl spray flames from the perspective of flame topological structure, filling the current gap in this field. More importantly, it can provide guidance for the design of combustion chambers in direct liquid ammonia injection gas turbines.

CRediT authorship contribution statement

Ruixiang Wang: Obtained data, Analyzed data, Performed research, Wrote the paper. **Meng Zhang:** Designed research, Revised the paper, Financial support, Supervision. **Zhenhua An:** Analyzed data, Figure production. **Xiao Cai:** Analyzed data, Technical support. **Jiawen Liu:** Obtained data, Performed research. **Jinhua Wang:** Financial support, Supervision. **Zuohua Huang:** Experimental and numerical configuration support.

Declaration of competing interest

The authors declare that they have no known competing financial interests or personal relationships that could have appeared to influence the work reported in this paper.

Acknowledgments

References

[1] A. Valera-Medina, H. Xiao, M. Owen-Jones, W.I. David, P. Bowen, Ammonia for power, Prog. Energy Combust. Sci. 69 (2018) 63–102.

[2] H. Kobayashi, A. Hayakawa, K.K.A. Somarathne, E.C. Okafor, Science and technology of ammonia combustion, Proc. Combust. Inst. 37 (1) (2019) 109–133.

[3] A. Hayakawa, Y. Arakawa, R. Mimoto, K.K.A. Somarathne, T. Kudo, H. Kobayashi, Experimental investigation of stabilization and emission characteristics of ammonia/air premixed flames in a swirl combustor, Int. J. Hydrog. Energy 42 (19) (2017) 14010–14018.

[4] X. Wei, M. Zhang, Z. An, J. Wang, Z. Huang, H. Tan, Large eddy simulation on flame topologies and the blow-off characteristics of ammonia/air flame in a model gas turbine combustor, Fuel 298 (2021) 120846.

[5] X. Wei, M. Zhang, J. Wang, Z. Huang, Investigation on lean blow-off characteristics and stabilization mechanism of premixed hydrogen enhanced ammonia/air swirl flames in a gas turbine combustor, Combust. Flame 249 (2023) 112600.

[6] O. Kurata, N. Iki, T. Matsunuma, T. Inoue, T. Tsujimura, H. Furutani, H. Kobayashi, A. Hayakawa, Performances and emission characteristics of NH3–air and NH3CH4–air combustion gas-turbine power generations, Proc. Combust. Inst. 36 (3) (2017) 3351–3359.

[7] M. Zhang, Z. An, L. Wang, X. Wei, B. Jianayihan, J. Wang, Z. Huang, H. Tan, The regulation effect of methane and hydrogen on the emission characteristics of ammonia/air combustion in a model combustor, Int. J. Hydrog. Energy 46 (40) (2021) 21013–21025.

[8] A.A. Khateeb, T.F. Guiberti, G. Wang, W.R. Boyette, M. Younes, A. Jamal, W.L. Roberts, Stability limits and NO emissions of premixed swirl ammonia-air flames enriched with hydrogen or methane at elevated pressures, Int. J. Hydrog. Energy 46 (21) (2021) 11969–11981.

[9] M.C. Franco, R.C. Rocha, M. Costa, M. Yehia, Characteristics of NH3/H2/air flames in a combustor fired by a swirl and bluff-body stabilized burner, Proc. Combust. Inst. 38 (4) (2021) 5129–5138.

[10] A.M. Elbaz, A.M. Albalawi, S. Wang, W.L. Roberts, Stability and characteristics of NH3/CH4/air flames in a combustor fired by a double swirl stabilized burner, Proc. Combust. Inst. 39 (4) (2023) 4205–4213.

[11] R. Pelé, C. Mounaïm-Rousselle, P. Bréquigny, C. Hespel, J. Bellettre, First study on ammonia spray characteristics with a current GDI engine injector, Fuels 2 (3) (2021) 253–271.

[12] Y. Fan, M. Ohtomo, S. Kasuga, N. Iki, O. Kurata, T. Tsujimura, H. Furutani, Characteristics of ammonia spray injected by pressure-swirl atomizers, in: International Conference on Liquid Atomization and Spray Systems, Vol. 1, no. 1, ICLASS, 2021.

[13] S. Li, T. Li, N. Wang, X. Zhou, R. Chen, P. Yi, An investigation on near-field and far-field characteristics of superheated ammonia spray, Fuel 324 (2022) 124683.

[14] X. Liu, X. Yao, Z. Wang, C. Tang, Single hole ammonia spray macroscopic and microscopic characteristics at flare and transition flash boiling regions, Appl. Therm. Eng. 235 (2023) 121443.

[15] S. Colson, H. Yamashita, K. Oku, K.K.A. Somarathne, T. Kudo, A. Hayakawa, H. Kobayashi, Study on the effect of injection temperature and nozzle geometry on the flashing transition of liquid ammonia spray, Fuel 348 (2023) 128612.

[16] E.C. Okafor, H. Yamashita, A. Hayakawa, K.K.A. Somarathne, T. Kudo, T. Tsujimura, M. Uchida, S. Ito, H. Kobayashi, Flame stability and emissions characteristics of liquid ammonia spray co-fired with methane in a single stage swirl combustor, Fuel 287 (2021) 119433.

[17] E.C. Okafor, O. Kurata, H. Yamashita, T. Inoue, T. Tsujimura, N. Iki, A. Hayakawa, S. Ito, M. Uchida, H. Kobayashi, Liquid ammonia spray combustion in two-stage micro gas turbine combustors at 0.25 MPa; Relevance of combustion enhancement to flame stability and NOx control, Appl. Energy Combust. Sci. 7 (2021) 100038.

[18] K.K.A. Somarathne, H. Yamashita, S. Colson, K. Oku, K. Honda, E.C. Okafor, A. Hayakawa, T. Kudo, H. Kobayashi, Towards the development of liquid ammonia/air spray combustion in a gas turbine-like combustor at moderately high pressure, Appl. Energy Combust. Sci. 16 (2023) 100215.

[19] M. UCHIDA, S. ITO, T. SUDA, Demonstration of direct spray combustion of liquid ammonia by 2MW-class gas turbine, in: The Proceedings of the International Conference on Power Engineering, ICOPE, 2021, p. 0250.

[20] H. Yamashita, E.C. Okafor, S. Colson, K.K.A. Somarathne, T. Tsujimura, S. Ito, M. Uchida, T. Kudo, A. Hayakawa, H. Kobayashi, Optical measurements under non-reacting condition and investigation of combustion characteristics in a swirling flow for liquid ammonia spray combustion, in: Japanese Symposium on Combustion, vol. 59th, (no. F0960C) 2021, p. B311.

[21] A.L. Sánchez, J. Urzay, A. Liñán, The role of separation of scales in the description of spray combustion, Proc. Combust. Inst. 35 (2) (2015) 1549–1577.

[22] A. Verdier, J.M. Santiago, A. Vandel, G. Godard, G. Cabot, B. Renou, Local extinction mechanisms analysis of spray jet flame using high speed diagnostics, Combust. Flame 193 (2018) 440–452.

[23] O.I. Awad, B. Zhou, K. Harrath, K. Kadirgama, Characteristics of NH3/H2 blend as carbon-free fuels: A review, Int. J. Hydrog. Energy 48 (96) (2023) 38077–38100.

[24] M. Aldén, Spatially and temporally resolved laser/optical diagnostics of combustion processes: From fundamentals to practical applications, Proc. Combust. Inst. 39 (1) (2023) 1185–1228.